

Cross sections of the reaction $^{231}\text{Pa}(d,3n)^{230}\text{U}$ for the production of $^{230}\text{U}/^{226}\text{Th}$ for targeted α therapyA. Morgenstern,^{1,*} O. Lebeda,² J. Stursa,² R. Capote,³ M. Sin,⁴ F. Bruchertseifer,¹ B. Zielinska,^{1,†} and C. Apostolidis¹¹European Commission, Joint Research Centre, Institute for Transuranium Elements, Post Office Box 2340, D-76125 Karlsruhe, Germany²Nuclear Physics Institute of the Academy of Sciences of the Czech Republic, Public Research Institution, CZ-250 68 Rez, Czech Republic³NAPC-Nuclear Data Section, International Atomic Energy Agency, A-1400 Vienna, Austria⁴Nuclear Physics Department, University of Bucharest, Post Office Box MG-11, RO-70709 Bucharest-Magurele, Romania

(Received 23 September 2009; published 25 November 2009)

^{230}U and its daughter nuclide ^{226}Th are novel therapeutic nuclides for application in targeted α therapy of cancer. We investigated the feasibility of producing $^{230}\text{U}/^{226}\text{Th}$ via deuteron irradiation of ^{231}Pa according to the reaction $^{231}\text{Pa}(d,3n)^{230}\text{U}$. The experimental excitation function for a deuteron-induced reaction on ^{231}Pa is reported for the first time. Cross sections were measured using thin targets of ^{231}Pa prepared by electrodeposition and ^{230}U yields were analysed using α spectrometry. Beam energies were calculated from measured beam orbits and compared with the values obtained via monitor reactions on aluminium foils using high-resolution γ spectrometry and IAEA recommended cross sections. Beam intensities were determined using a beam current integrator. The experimental cross sections are in excellent agreement with model calculations allowing for deuteron breakup using the EMPIRE 3 code. According to thick-target yields calculated from the experimental excitation function, the reaction $^{231}\text{Pa}(d,3n)^{230}\text{U}$ allows the production of $^{230}\text{U}/^{226}\text{Th}$ at moderate levels.

DOI: [10.1103/PhysRevC.80.054612](https://doi.org/10.1103/PhysRevC.80.054612)

PACS number(s): 25.45.-z, 24.10.-i, 87.57.un

I. INTRODUCTION

The α emitter ^{230}U ($T_{1/2} = 20.8$ d) and its daughter nuclide ^{226}Th ($T_{1/2} = 31$ min) are novel therapeutic nuclides for application in targeted α therapy (TAT) of cancer [1,2]. Both α emitters decay through a cascade of further α -emitting daughter nuclides, generating a highly cytotoxic dose to targeted cancer cells. For application of the novel α emitters in TAT, the production of $^{230}\text{U}/^{226}\text{Th}$ in clinically relevant amounts is a main prerequisite. We have recently reported two cyclotron-driven processes for the production of $^{230}\text{U}/^{226}\text{Th}$, based on proton irradiation of ^{232}Th or ^{231}Pa [1,2]. Both processes allow the production of the therapeutic nuclides in carrier-free form at clinically relevant levels. The currently most frequently used process for the production of $^{230}\text{U}/^{226}\text{Th}$ is based on proton irradiation of natural ^{232}Th according to the reaction $^{232}\text{Th}(p,3n)^{230}\text{Pa}$. Following the β^- decay of ^{230}Pa ($T_{1/2} = 17.4$ d, 8.4% branching), carrier-free ^{230}U can be isolated from the irradiated target four weeks after the end of bombardment (EOB) with a maximum activity of 2.8% relative to the activity of ^{230}Pa initially produced. The maximum cross section for the reaction $^{232}\text{Th}(p,3n)^{230}\text{Pa}$ was reported as 353 ± 14.5 mb at 19.9 ± 0.3 MeV proton energy. The production process is technically relatively simple and allows the production of ^{230}Pa with thick-target yields of 8.4 MBq/ $\mu\text{A} \cdot \text{h}$ at 33.5 MeV, resulting in 0.24 MBq/ $\mu\text{A} \cdot \text{h}$ of ^{230}U at 28 days after EOB.

However, as ^{230}U is produced in this process in an indirect manner via the intermediate nuclide ^{230}Pa , we hypothesized that alternative nuclear reactions leading directly to the desired nuclide ^{230}U could potentially increase production yields. In this respect, the nuclide ^{231}Pa ($T_{1/2} = 32760$ yr), available in gram quantities from the ^{235}U decay chain, presents a suitable target material for the reactions $^{231}\text{Pa}(p,2n)^{230}\text{U}$ and $^{231}\text{Pa}(d,3n)^{230}\text{U}$. As we have recently reported, the maximum cross section for the reaction $^{231}\text{Pa}(p,2n)^{230}\text{U}$ was found as 33.2 ± 5.3 mb at 14.6 ± 0.2 MeV proton energy, in very good agreement with model calculations using the EMPIRE 3 code [2]. Although this cross section is approximately one order of magnitude lower than the cross section for the reaction $^{232}\text{Th}(p,3n)^{230}\text{Pa}$, the thick-target yield for the proton irradiation of ^{231}Pa was found to be comparable at 0.25 MBq/ $\mu\text{A} \cdot \text{h}$, calculated for the energy loss of $24 \rightarrow 10.5$ MeV, due to the direct pathway of production.

With respect to deuteron-induced reactions on ^{231}Pa , our survey of literature data did not yield any relevant cross-section data. Consequently, to investigate the productivity of the reaction $^{231}\text{Pa}(d,3n)^{230}\text{U}$, we have measured the excitation function of the reaction in the energy range of interest for production of ^{230}U . In addition to its relevance for radionuclide production, the first measurement of the $^{231}\text{Pa}(d,3n)$ reaction is also important as a benchmark of the modeling of deuteron-induced nuclear reactions on heavy targets. Fission is the dominant decay channel for these nuclei, but additional data on neutron emission further constrain nuclear model parameters, thereby increasing the reliability of theoretical calculations. Moreover, a proper description of obtained experimental data is a tough benchmark for fission input parameters derived from the study of neutron-induced fission of $^{233-231}\text{U}$ isotopes.

*Corresponding author: alfred.morgenstern@ec.europa.eu

†Present address: Department of Radiochemistry, Institute of Nuclear Chemistry and Technology, Dorodna 16, PL-03-195, Warsaw, Poland.

II. EXPERIMENT

A. Sample preparation, irradiation conditions, and beam energy monitoring

Solutions of hydrochloric acid and hydrofluoric acid were prepared from suprapur grade reagents (Merck). Water was obtained from a Milli-Q water purification system. ^{231}Pa was obtained as Pa_2O_5 from the chemistry division of AERE Harwell. All other chemicals were reagent grade and were used as received.

The purification of the ^{231}Pa stock solution and the preparation of thin targets of ^{231}Pa by electrodeposition on silver disks have been described previously [2]. During electrodeposition a hole mask of 9 mm diameter was used to obtain protactinium layers of defined geometry containing 14.2 to 16.1 μg of ^{231}Pa . The homogeneity of the ^{231}Pa layers was assessed by autoradiography (Molecular Imager FX, Bio-Rad) and analyzed using the QUANTITY ONE software (Bio-Rad). Targets were used for cross-section measurements if maximum variations in the thickness of ^{231}Pa layers across the circular area were found to be less than 10%. Subsequently the silver disks were covered with aluminium foils (34.9 μm thickness, 99.99%, Alfa Aesar) acting as catcher foils to avoid any losses of activity by recoil processes.

Irradiations were performed at the isochronous cyclotron U-120M of the Nuclear Physics Institute in Rez, Czech Republic. Deuteron irradiations of thin ^{231}Pa targets were performed at incident energies of 11.2–19.9 MeV using currents of 4.7–6.4 μA for 4–6 h. During irradiations, a beam collimator of 8.5 mm diameter was used to focus the beam on the protactinium layer of 9 mm diameter and the backside of the targets was cooled with water. Aluminium foils of 21.0 μm thickness (99.99%, Alfa Aesar) used as monitor foils were irradiated immediately before sample irradiation at identical beam positions and in identical position as the targets.

Beam intensities were determined by using a beam current integrator. Beam energies extracted from the cyclotron were determined from the beam orbit position measurements. The energy calculation was based on the cyclotron model described by Cihak *et al.* [3]. The energies entering the protactinium target layers were calculated using the SRIM 2003 code [4] by taking into account the loss of deuteron energy in the cover foils. Deuteron beam energies were also monitored based on the $^{27}\text{Al}(d,x)^{24}\text{Na}$ monitor reaction using IAEA updated recommended cross-section data [5]. Decay data for ^{24}Na ($T_{1/2} = 14.959$ h, $E_\gamma = 1\,368.63$ keV, $I_\gamma = 100\%$) were taken from Firestone *et al.* [6].

B. Measurement of radioactivity

High-resolution γ spectrometry (HRGS) of activated monitor foils was performed using a γ spectrometer equipped with a HPGe detector (GMX45-Plus, FWHM 2.04 keV at 1332.5 keV, amplifier 671, ADC TRUMP-8 K-IN LINE, multichannel analyzer TRUMP-8 K, software MAESTRO for Windows; Ortec). The spectrometer was calibrated for absolute counting efficiency with a set of γ -ray standards (^{152}Eu , ^{137}Cs , ^{60}Co , ^{133}Ba , and ^{241}Am , uncertainty of the activities <1%, Czech Institute for Metrology, Department

of Ionizing Radiation) for various geometries. In the energy range 240–1408 keV, where the logarithm of efficiency is a linear function of the logarithm of energy, the square of the correlation coefficient of all linear fits was higher than 0.999. Differences between measured and fitted efficiency values did not exceed 2% for any γ line used for the calibration. Net peak areas of the standard γ lines used for the calibration were kept over 10^6 counts.

The activity measurement of ^{230}Pa and ^{230}U in individual thin foils was performed by α spectrometry (Soloist, EG&G Ortec). The efficiency of the α detector was calibrated using a mixed $^{239}\text{Pu}/^{241}\text{Am}/^{244}\text{Cm}$ standard (AMR43, Amersham). Counting times were set to reach at least 10^4 counts in each region of interest.

Aluminium cover foils were removed from the silver target foils containing the $^{231}\text{Pa}/^{230}\text{U}$ layer and both foils were measured by α spectrometry. The direct α spectrometric measurement of the activated silver target foils resulted in α spectra of low resolution and did not allow the determination of the activities of ^{231}Pa and ^{230}U because of spectral interferences. Consequently, the activated layers were dissolved by stepwise addition of $8 \times 50 \mu\text{l}$ of 4.5 M hydrochloric acid/0.1 M hydrofluoric acid with a yield ranging from 80% to 100%. An aliquot of the resulting solution was added onto a new silver disk to prepare samples for α spectrometry by evaporation. The residual silver target foils were dried and also counted by α spectrometry. This procedure led to α spectra of high resolution, as illustrated in Fig. 1, which shows a typical α spectrum obtained from a ^{231}Pa target irradiated with deuterons of 16.1 MeV energy. Decay data for the α emissions of ^{231}Pa , ^{230}U , and their daughter nuclides are taken from Ref. [7] and summarized in Table I. Because of spectral interferences between the α emissions of ^{230}U and $^{227}\text{Th}/^{223}\text{Ra}$ generated through the decay of ^{231}Pa , the activity of ^{230}U was determined via analysis of the α emission of its daughter nuclide ^{214}Po at 7.7 MeV after radioactive equilibrium was reached.

C. Calculation of cross sections and uncertainty determination

Cross sections were calculated using the activation equation based on beam current, target thickness, and reaction product

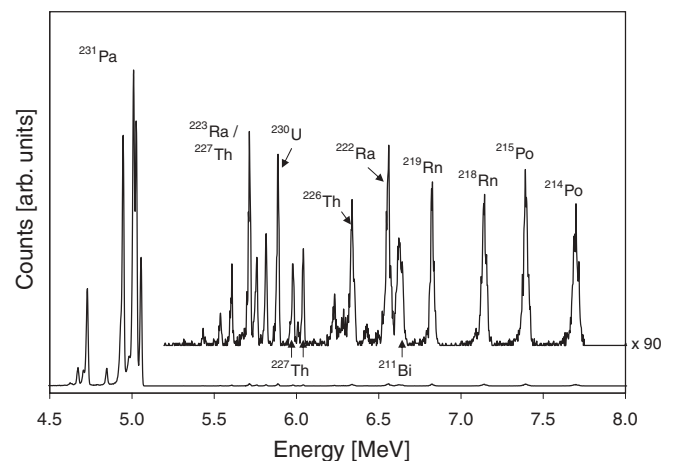


FIG. 1. α spectrum of ^{231}Pa after irradiation with deuterons at 16.1 MeV. The inset is magnified 90 times.

TABLE I. Principal α emissions (emission probability >0.1) of ^{231}Pa , ^{230}U , and their α -particle-emitting daughter nuclides [7].

Nuclide	Half-life	Energy (MeV)	Emission probability	Nuclide	Half-life	Energy (MeV)	Emission probability		
^{231}Pa	32 760 yr	5.014	0.254	^{230}U	20.8 d	5.888	0.674		
		4.951	0.229			5.818	0.320		
		5.030	0.200	^{226}Th	30.6 min	6.337	0.755		
		5.059	0.110			6.234	0.228		
^{227}Th	18.72 d	6.038	0.242	^{222}Ra	38 s	6.559	0.969		
		5.978	0.235			^{218}Rn	35 ms	7.129	0.999
		5.757	0.204					^{214}Po	164 μs
^{223}Ra	11.43 d	5.716	0.525						
		5.607	0.242						
^{219}Rn	3.96 s	6.819	0.808						
		6.553	0.115						
^{215}Po	1.78 ms	7.386	0.999						
^{211}Bi	2.17 min	6.623	0.834						
		6.279	0.164						

activity. There are several major contributions to the overall uncertainty of the determined cross sections: the uncertainty of beam current measurement, which is given by the uncertainty of the beam current integrator ($<5\%$), the uncertainty in the thickness of the ^{231}Pa target layer ($<10\%$), and the uncertainty in determining the activity of ^{230}U including the uncertainty of its decay data ($<5\%$) [6]. The uncertainty associated with dissolution of the ^{231}Pa target layer and preparation of new samples for α spectrometric measurements is mainly related to the measurement of the volume of the resulting solution ($<2\%$) and possible losses of activity during sample evaporation, which are considered to be negligible. The overall uncertainty in the determination of the ^{230}U cross sections was thus $<12.3\%$.

The uncertainty of the beam energy determined from the beam orbit position measurements and calculated from the mathematical cyclotron model ranges from 100 to 200 keV. This corresponds to $<2.0\%$ for 10 MeV and $<1.0\%$ for 20 MeV. The correlation between the deuteron energy determined in this way and that calculated from the activation of the aluminium monitor was excellent, with a correlation coefficient of >0.998 . Since the uncertainty of the former method is lower, we adopted the energies calculated from the beam orbit positions as conventionally true. The paired t test showed that at the 0.95% confidence level, the results of the two methods differ: The monitor gives systematically slightly lower energy than the beam orbit position. This might be due to both the recommended cross section data for the monitor reaction and a possible systematic error in the beam current measurement. However, the systematic shift is very small (0.20 MeV on average).

III. NUCLEAR MODEL CALCULATIONS

The theoretical prediction of the $^{231}\text{Pa}(d,3n)$ cross section was undertaken with the modular system EMPIRE 3 [8–11], which uses updated nuclear reaction models to describe the direct, pre-equilibrium, and compound-nucleus reaction

mechanisms relevant to the studied energy range. Direct reaction processes play a very significant role in the description of deuteron-induced reactions near the Coulomb barrier; in particular, the deuteron breakup significantly reduces the available compound-nucleus cross section and increases the expected proton emission by almost two orders of magnitude in comparison with the proton statistical emission. Direct reactions induced by incident deuterons were estimated by Kalbach's parametrization [12].

The Daechnick spherical optical model potential for deuterons [13] (RIPL 6116) was used for the incident and inelastic deuteron channels. The particle transmission coefficients for the emerging nucleon channels were calculated using the dispersive nucleon potential developed for actinides [14] (RIPL 2408 and RIPL 5408 for neutrons and protons, respectively). All the optical model calculations were performed with the ECIS06 code [15] incorporated into the EMPIRE 3 system. Pre-equilibrium emission was taken into account by the module PCROSS based on the one-component exciton model with γ , nucleon, α , and deuteron emissions. For the calculations of the compound nucleus cross sections the full featured Hauser-Feshbach (HF) statistical model was used. Deuteron-induced fission of ^{231}Pa is the dominant reaction channel; therefore, the employed HF statistical model includes decay probabilities deduced in the optical model for fission [16,17] and accounts for the multiple-particle emission and the full γ cascade.

An accurate theoretical prediction requires, in addition to quality nuclear models, an appropriate set of input parameters. The model parameters deduced in our previous study of the $p + ^{231}\text{Pa}$ reaction [2] were used as starting values for the input parameters of the nuclear model calculations. Additional required parameters were retrieved from the RIPL-2 database [18].

Input parameters may be adjusted within their estimated uncertainties in the evaluation process to describe simultaneously all the observables. In this respect, the calculations

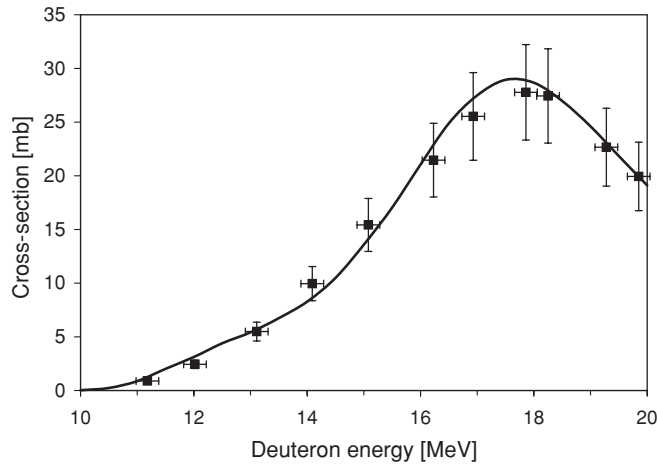


FIG. 2. Experimentally determined cross sections for the reaction $^{231}\text{Pa}(d,3n)^{230}\text{U}$ in comparison with model calculations using the EMPIRE 3 code.

presented in this work represented a challenge, because no direct experimental data for the competing channels were available that could be used in constraining the choice of parameters. Moreover, deuteron energies of interest for this study were below the Coulomb barrier, which is estimated to be around 20 MeV for the system $d + ^{231}\text{Pa}$. Fortunately, the EMPIRE 3 system has been previously used on a large number of actinides [11,19,20] to test the validity of available sets of global level densities for normal and transition states, deduced from a phenomenological basis [10]. This experience allowed us to choose for the most important parameters and model those with the best predictive power. Among them, we should mention the enhanced generalized superfluid model (EGSM) [10] used in the calculation of the required nuclear level densities. For consistency with the ground state, the level

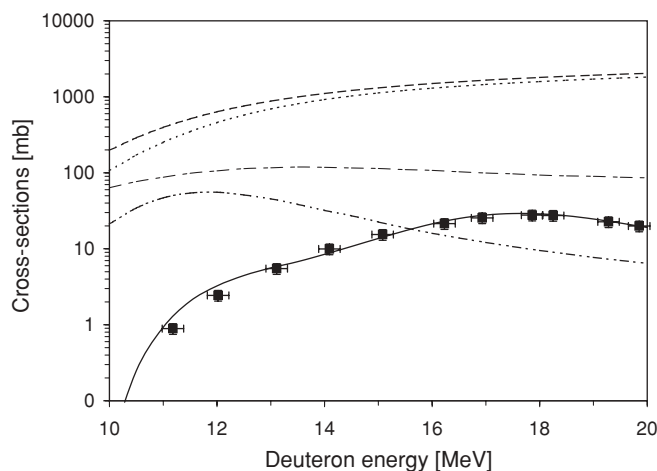


FIG. 3. Theoretically calculated deuteron-induced cross sections on ^{231}Pa for major competing reactions as obtained by the EMPIRE 3 code. The solid line corresponds to the $(d,3n)$ reaction, the long dashed line corresponds to the overall reaction cross section (cumulative cross section of all reaction channels), the dashed line to the fission cross section, the dot-dashed line to proton emission, and the double dot-dashed line to the $(d,2n)$ reaction.

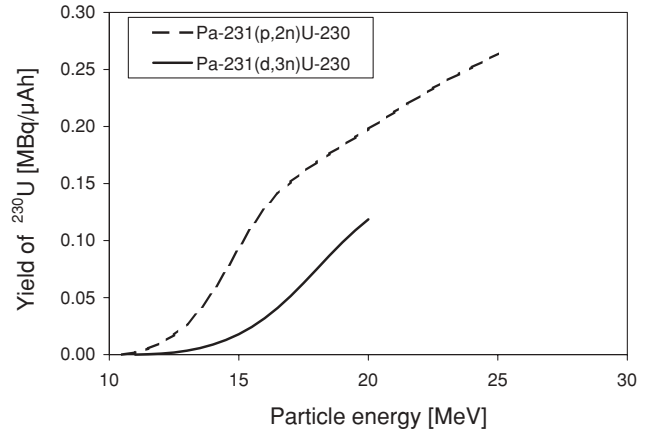


FIG. 4. Thick-target yield of ^{230}U produced via the $^{231}\text{Pa}(d,3n)^{230}\text{U}$ reaction in $^{231}\text{Pa}_2\text{O}_5$ (density 9.10 g/cm^3) calculated from the experimental excitation function presented in this work for $E_{\text{out}} = 11.0\text{ MeV}$. For comparison the thick-target yield of ^{230}U produced via the $^{231}\text{Pa}(p,2n)^{230}\text{U}$ reaction is shown calculated for $E_{\text{out}} = 10.5\text{ MeV}$ from the experimental excitation function reported in Ref. [2].

densities at saddles were also calculated using the EGSM, but with parameters and enhancement factors specific to the corresponding deformations of the nuclear shape.

Special attention was paid to fission, which is the dominant reaction channel in the energy range of interest for this work. The fission barrier parameters for $^{233,232,231,230}\text{U}$ were chosen based on EMPIRE systematics, slightly adjusted to reproduce the trend of the HFB global microscopic calculations [20,21] and the evaluations of the neutron-induced fission on the light uranium isotopes [22].

IV. RESULTS AND DISCUSSION

The experimentally determined cross sections for the reaction $^{231}\text{Pa}(d,3n)^{230}\text{U}$ are summarized in Table II and shown in Fig. 2. This excitation function has been measured for the first time. The maximum of the $^{231}\text{Pa}(d,3n)^{230}\text{U}$ excitation function ($27.8 \pm 3.4\text{ mb}$) was found at $17.9 \pm 0.2\text{ MeV}$ deuteron energy.

TABLE II. Experimental cross sections for the reaction $^{231}\text{Pa}(d,3n)^{230}\text{U}$.

Energy (MeV)	Cross section (mb)
11.2 ± 0.2	0.89 ± 0.11
12.0 ± 0.2	2.44 ± 0.30
13.1 ± 0.2	5.49 ± 0.67
14.1 ± 0.2	9.95 ± 1.22
15.1 ± 0.2	15.4 ± 1.9
16.2 ± 0.2	21.5 ± 2.6
16.9 ± 0.2	25.5 ± 3.1
17.9 ± 0.2	27.8 ± 3.4
18.3 ± 0.2	27.4 ± 3.4
19.3 ± 0.2	22.7 ± 2.8
19.9 ± 0.2	19.9 ± 2.4

TABLE III. Comparison of the production routes for ^{230}U and their yields.

Reaction	Max. cross section (mb)	Thick-target yield (MBq/ $\mu\text{A} \cdot \text{h}$)	Ref.
$^{231}\text{Pa}(d,3n)^{230}\text{U}$	27.8 ± 3.4 (17.9 MeV)	0.119 (20.0 \rightarrow 11.0 MeV, oxide)	This work
$^{231}\text{Pa}(p,2n)^{230}\text{U}$	33.2 ± 5.3 (14.6 MeV)	0.245 (24.0 \rightarrow 10.5 MeV, oxide)	[2]
$^{232}\text{Th}(p,3n)^{230}\text{Pa}(\beta^-)^{230}\text{U}$	353 ± 15 (19.9 MeV)	8.4^a (33.5 MeV)	[1]

^aThick-target yield of ^{230}Pa . The maximum activity of ^{230}U is formed four weeks after the end of irradiation via β^- decay of ^{230}Pa and corresponds to 2.82% of the activity of ^{230}Pa initially produced. The available amount of ^{230}U thus corresponds to a yield of 0.24 MBq/ $\mu\text{A} \cdot \text{h}$.

This value is slightly lower than the maximum cross section for the $(p,2n)$ reaction (33.2 ± 5.3 mb at 14.6 ± 0.2 MeV) [2]. Although the excitation function for the $(d,3n)$ reaction could not be measured in the full range owing to the limited deuteron energies available at the U-120 M cyclotron (≤ 20 MeV), the shape of the excitation function including the maximum is clearly visible.

The results of nuclear model calculations for the $(d,3n)$ reaction using the EMPIRE 3 code are also included in Fig. 2. The agreement with the experimental data is excellent, showing the reliability and consistency of the employed model and the input parameters for proper treatment of fission and neutron and proton emission. In Fig. 3 the calculated cross sections for the major reactions induced by deuterons in ^{231}Pa are shown. We can see that the deuteron-induced fission is always two orders of magnitude higher than the studied $(d,3n)$ reaction, making the proper description of fission below the Coulomb barrier a prerequisite for modeling the reaction of interest. The contribution of proton emission (~ 100 mb) is almost independent of the incident deuteron energy. A comprehensive description of the theoretical modeling of charged-particle-induced reactions for the production of ^{230}U and corresponding neutron-induced fission reactions leading to the same compound nuclei will be published elsewhere.

Based on the cross sections experimentally determined in this work, thick-target yields for the production of ^{230}U by deuteron irradiation of ^{231}Pa were calculated (Fig. 4). The

thick-target yield was found to be 0.119 MBq/ $\mu\text{A} \cdot \text{h}$ for the energy loss $20 \rightarrow 11.0$ MeV in a thick target made from protactinium oxide, a value that is considerably lower than the thick-target yield determined for the $(p,2n)$ reaction (0.245 MBq/ $\mu\text{A} \cdot \text{h}$, $24.0 \rightarrow 10.5$ MeV, oxide) [2]. Table III gives a summary of the nuclear reactions reported so far for the production of ^{230}U . If one assumes a therapeutic dose of 5–10 MBq of ^{230}U required for patient treatment [1,2], all three processes allow the production of ^{230}U at levels sufficient for patient treatment. However, the process based on proton irradiation of natural ^{232}Th seems favorable for large-scale, routine production because of high production yields and the ease of preparation and handling of targets made from natural, long half-life ^{232}Th . Because the production of targets made from ^{231}Pa is more complex, the main advantage of the reaction $^{231}\text{Pa}(p,2n)^{230}\text{U}$ is that it can be performed at smaller cyclotrons with proton energies below 25 MeV. The reaction $^{231}\text{Pa}(d,3n)^{230}\text{U}$ investigated in this work offers the lowest thick-target yields and requires larger accelerators offering deuteron beams of up to 30 MeV to utilize the full integral of the excitation function.

ACKNOWLEDGMENTS

EMPIRE 3 cross-section calculations involved a version of the code that has been under development for many years as a multinational effort under the leadership of Mike Herman.

- [1] A. Morgenstern, C. Apostolidis, F. Bruchertseifer, R. Capote, T. Gouder, F. Simonelli, M. Sin, and K. Abbas, *Appl. Radiat. Isotopes* **66**, 1275 (2008).
- [2] A. Morgenstern, O. Lebeda, J. Stursa, F. Bruchertseifer, R. Capote, J. McGinley, G. Rasmussen, M. Sin, B. Zielinska, and C. Apostolidis, *Anal. Chem.* **80**, 8763 (2008).
- [3] M. Cihák, O. Lebeda, and J. Štursa, in *Proceedings of the 18th Interantional Conference on Cyclotrons and Applications, CYCLOTRONS 2007* (Giardini Naxos, Italy, 2007).
- [4] J. F. Ziegler, J. P. Biersack, and U. Littmark, *SRIM 2003 Code. The Stopping and Range of Ions in Solids* (Pergamon, New York, 2003).
- [5] IAEA, Charged-Particle Cross Section Database for Medical Radioisotope Production, http://www-nds.iaea.org/medical/monitor_reactions.html (update of March 2007).
- [6] R. B. Firestone, C. M. Baglin, and F. S. Y. Chu, *Table of Isotopes*, 8th ed. (Wiley, New York, 1998). Update on CD-ROM.
- [7] Nucleonica—Web driven nuclear science, European Commission, Joint Research Centre, Institute for Transuranium Elements (2007), <http://www.nucleonica.net/index.aspx>, <http://www.nucleonica.net/index.aspx>.
- [8] M. Herman, in *Nuclear Reaction Data and Nuclear Reactors*, edited by N. Paver, M. Herman and A. Gandini, Vol. 5 of ICTP Lecture Notes (ICTP, Trieste, 2001). pp. 137–230.
- [9] M. Herman, P. Oblozinsky, R. Capote, M. Sin, A. Trkov, A. Ventura, and V. Zerkin, in *Proceedings of the International Conference on Nuclear Data for Science and Technology, 26 September–1 October 2004, Santa Fe, New Mexico, USA*, AIP Conf. Proc. (American Institute of Physics, Melville, New York, 2005), Vol. 769.
- [10] M. Herman, R. Capote, B. V. Carlson, P. Oblozinsky, M. Sin, A. Trkov, H. Wienke, and V. Zerkin, *Nucl. Data Sheets* **108**, 2655 (2007).

- [11] R. Capote, M. Sin, A. Trkov, M. Herman, B. V. Carlson, and P. Oblozinsky, in *Proceedings of the International Conference on Nuclear Data for Science and Technology, 22–27 April 2007, Nice, France*, edited by O. Bersillon, F. Gunsing, E. Bauge, R. Jacqmin, and S. Leray (EDP Sciences, Les Ulis, France, 2007), available online at <http://dx.doi.org/10.1051/ndata:07755>.
- [12] C. Kalbach, PRECO2000 code, available online at <http://www.nndc.bnl.gov/nndcscr/model-codes/preco-2000/preco-2000.zip>.
- [13] W. W. Daehnick, J. D. Childs, and Z. Vrcelj, *Phys. Rev. C* **21**, 2253 (1980).
- [14] R. Capote, E. Sh. Soukhovitskii, J. M. Quesada, and S. Chiba, in *Proceedings of the International Conference on Nuclear Data for Science and Technology, 22–27 April 2007, Nice, France*, edited by O. Bersillon, F. Gunsing, E. Bauge, R. Jacqmin, and S. Leray (EDP Sciences, Les Ulis, France, 2007), available online at <http://dx.doi.org/10.1051/ndata:07765>.
- [15] J. Raynal, in *Computing as a Language of Physics, ICTP International Seminar Course, Trieste, Italy, 2–10 August 1971* (IAEA, Vienna, 1972), p. 281.
- [16] M. Sin, R. Capote, A. Ventura, M. Herman, and P. Oblozinsky, *Phys. Rev. C* **74**, 014608 (2006).
- [17] M. Sin, and R. Capote, *Phys. Rev. C* **77**, 054601 (2008).
- [18] T. Belgya, O. Bersillon, R. Capote, T. Fukahori, G. Zhigang, S. Goriely, M. Herman, A. V. Ignatyuk, S. Kailas, A. Koning, P. Oblozinsky, V. Plujko, and P. Young, *Handbook for Calculations of Nuclear Reaction Data, RIPL-2*, IAEA-TECDOC-1506 (IAEA, Vienna, 2006), available online at <http://www-nds.iaea.org/RIPL-2/>.
- [19] R. Capote, M. Sin, and A. Trkov, documentation of the Th-232 Evaluation for ENDF/B-VII.0 (MAT = 9040 MF = 1 MT = 451), National Nuclear Data Center, Brookhaven National Laboratory, 15 December 2006.
- [20] M. Sin, R. Capote, S. Goriely, S. Hilaire, and A. J. Koning, in *Proceedings of the International Conference on Nuclear Data for Science and Technology, 22–27 April 2007, Nice, France*, edited by O. Bersillon, F. Gunsing, E. Bauge, R. Jacqmin, and S. Leray (EDP Sciences, Les Ulis, France, 2008), available online at <http://dx.doi.org/10.1051/ndata:07370>.
- [21] S. Goriely, and J. M. Pearson, in *Proceedings of the International Conference on Nuclear Data for Science and Technology, 22–27 April 2007, Nice, France*, edited by O. Bersillon, F. Gunsing, E. Bauge, R. Jacqmin, and S. Leray (EDP Sciences, Les Ulis, France, 2008), available online at <http://dx.doi.org/10.1051/ndata:07263>.
- [22] P. G. Young, M. B. Chadwick, R. E. MacFarlane, P. Talou, T. Kawano, D. G. Madland, W. B. Wilson, and C. W. Wilkerson, *Nucl. Data Sheets* **108**, 2589 (2007).